

## Wigner Crystallization in $(\text{DI-DCNQI})_2\text{Ag}$ Detected by Synchrotron Radiation X-Ray Diffraction

T. Kakiuchi,<sup>1</sup> Y. Wakabayashi,<sup>2</sup> H. Sawa,<sup>1,2,\*</sup> T. Itou,<sup>3,†</sup> and K. Kanoda<sup>3</sup>

<sup>1</sup>*Department of Materials Structure Science, The Graduate University for Advanced Studies, Tsukuba, Ibaraki 305-0801, Japan*

<sup>2</sup>*Institute of Materials Structure Science, High Energy Accelerator Research Organization, Tsukuba, Ibaraki 305-0801, Japan*

<sup>3</sup>*Department of Applied Physics, University of Tokyo, Bunkyo-ku, Tokyo 113-8656, Japan*

(Received 20 September 2006; published 6 February 2007)

The low-temperature electronic structure of the quarter-filled, quasi-one-dimensional (Q1D) system  $(\text{DI-DCNQI})_2\text{Ag}$  is revealed using synchrotron radiation x-ray diffraction. In spite of the interchain frustration in the twofold superstructure along the 1D chain, the body-centered tetragonal “charge ordering” structure, which consists of  $4k_F$  charge ordering columns and  $4k_F$  bond order wave columns, is realized. This is the first example of the Q1D system having plural kinds of columns as its ground state. This charge ordered structure is regarded as a Wigner crystal caused by intercolumn Coulomb repulsion.

DOI: 10.1103/PhysRevLett.98.066402

PACS numbers: 71.30.+h, 61.66.Hq

One-dimensional metals are known to undergo a metal-insulator phase transition at low temperature, as first discussed by Peierls [1]. Presently, various electronic ground states of quarter-filled quasi-one-dimensional (Q1D) systems are understood theoretically in terms of a simple extended Hubbard model mainly using three electron correlation parameters  $t$ ,  $U$ , and  $V$  [2], where  $t$  is the transfer integral between nearest neighboring molecules, and  $U$  and  $V$  are the on-site and the intersite Coulomb energy, respectively. In this model, a variety of phases, e.g., spin-Peierls, spin density wave, and charge ordering (CO) phases, have been predicted as their ground state in certain  $U/t$  and  $V/t$  regions.

A  $(\text{DCNQI})_2\text{Ag}$  series is regarded as a model Q1D electron system. Since Ag is a monovalent ion having a closed shell, DCNQI molecules have a valence of  $-0.5$  on average and they construct a quarter-filled 1D- $\pi$ -electron band which consists of the lowest unoccupied molecular orbital. Ag contributes little to this band [3] because it is a stable closed-shell ion. One of the series,  $(\text{DMe-DCNQI})_2\text{Ag}$ , shows a metal-insulator transition and a spin-Peierls transition at 100 and 80 K, respectively [4,5]. Accompanied by these transitions, a  $4k_F$  charge density wave (CDW) and a  $2k_F$  CDW were established below 100 and 80 K, respectively, as observed by x-ray diffraction measurements [6,7]. These phenomena were regarded as characteristic of a one-dimensional system in which the Peierls instability plays an important and intrinsic role, although electron correlation also affects their ground states. By contrast,  $(\text{DI-DCNQI})_2\text{Ag}$  is insulating even at room temperature and exhibits an antiferromagnetic order at 5.5 K [5,8,9]. Below 220 K, Ref. [8] reported a clear split in the  $^{13}\text{C}$ -NMR spectrum and suggested that the  $4k_F$  Wigner crystal type of CO on DCNQI molecules arose in the low-temperature (LT) phase. This CO ground state on the 1D chain made by long-range Coulomb repulsion was predicted by mean field calculation within a

extended Hubbard model [10] in a large  $V/t$  and  $U/t$  region. It is very interesting whether (or how) the electron crystal is stable in the real solid which involves a periodic potential of lattice and electron-phonon interaction. In this Letter, we report the results of a crystal structure analysis of  $(\text{DI-DCNQI})_2\text{Ag}$  at low temperature using synchrotron x-ray diffraction by which we determined the 3D CO structure of this substance. Despite its complicated structure, the obtained CO arrangement is regarded as a simple Wigner crystal caused by Coulomb repulsion.

Single crystal x-ray diffraction measurements using x rays having a wavelength  $0.6870 \text{ \AA}$  were performed on an imaging plate Weissenberg camera installed on beam lines BL-1A and -1B at the Photon Factory, KEK, Japan. A four-circle diffractometer installed on BL-4C for high-resolution experiments was also used. The sample temperature was controlled by closed-cycle helium refrigerators. The sample was grown using the electrochemical method, and the size of the specimen used for structure analysis was  $0.35 \times 0.05 \times 0.05 \text{ mm}^3$ .

The crystal structure of  $(\text{DI-DCNQI})_2\text{Ag}$  at room temperature has been described as having a space group of  $I4_1/a$  [11]. Planer DCNQI molecules are piled up at even intervals along the  $c$  direction, composing one-dimensional columns. In this space group, the molecules are connected by the symmetrical operation of a fourfold screw whose axis runs parallel to the  $c$  axis and travels through the center of four substitution radicals (iodine), and inversion centers are located on every molecule and at the midpoint of two piled molecules. Ag on the  $\bar{4}$  axis is coordinated in local symmetry of  $D_{2d}$  distorted tetrahedral fashion to the N atoms in the DCNQI molecule.

At room temperature, diffuse scattering characterized by the wave vector  $e^*/2$  was observed, as has been previously reported [7]. The diffuse distribution of the scattering intensity gradually condensed into superlattice spots characterized by the wave vector  $(0\ 0\ \frac{1}{2})$  with decreasing tem-

perature. Although these superlattice spots spread slightly in the  $c^*$  plane even at 50 K, the three-dimensional correlation length was sufficiently long to allow a structure analysis; the correlation length was about 1300 Å along the  $a$  direction based on the peak profile measured using the four-circle diffractometer. The typical ratio of the intensity of superlattice reflections to that of fundamental reflections was  $10^{-3}$ . At 50 K, for crystal structure analysis we measured a data set that includes superlattice reflections. The primitive unit cell of the superstructure in the LT phase was found to be  $a_p \times b_p \times 2c_p$ , where  $a_p$ ,  $b_p$ , and  $c_p$  are lattice constants with the  $I4_1/a$  in the high-temperature (HT) phase. No systematic absence of superlattice reflections was found. If the Bravais lattice at the LT phase is tetragonal, only one space group of the  $2c_p$ -cell structure is possible within the limitations of the subgroup for  $I4_1/a$ :  $P4$ . However, this space group contradicts the experimental results of the persistence of inversion symmetry obtained by optical measurement [12,13]. Since there is no candidate having an inversion center in the tetragonal subgroups, the crystal system in the LT phase has to be monoclinic. In this case, the symmetry reduction from tetragonal to monoclinic must be accompanied by a twinning. We assumed a twinning structure which includes domains  $(a, b, c)$  and  $(b, -a, c)$  because of the transition from Laue class  $4/m$  to  $2/m$ . No peak split was observed within the instrumental resolution of  $0.05^\circ$ , indicating that the unit cell deformation is very small. The lattice parameters at 50 K, which were  $a = 22.346(5)$  Å,  $b = 22.346(5)$  Å,  $c = 7.984(2)$  Å,  $\gamma = 90^\circ$ , and  $V = 3986.8(16)$  Å<sup>3</sup>, hardly deviate from the tetragonal. In addition to this, the thermal expansion coefficient was nearly constant around the transition temperature. These results mean that the twinning's deformation energy is extremely small. The only monoclinic space group for the  $a_p \times b_p \times 2c_p$  structure that carries the inversion symmetry was  $P2/a$ , whose unique axis is  $c$ . The twinned crystal structure refinement [14] was performed using the full matrix least square method and converged, showing good reliability factors ( $R_{\text{all}} = 0.058$ , goodness of fit [15] was 1.129). The refined fraction of the two domains was 0.519(3):0.481. Figure 1 shows the structure and symmetrical operation of the LT phase. Three independent columns labeled A–C and four independent Ag ions labeled  $\underline{1}$ – $\underline{4}$  comprise the structure of the LT phase. Ag ions are placed on the twofold rotation axis. As shown in panel (b), the inversion centers are on the molecules in column A and at the midpoint of two molecules in column C, although there are no inversion centers on column B. Note that molecules 5 and 6 are equivalent.

The magnitude of the charge disproportionation among molecules is often estimated by deformation of molecules [16]. However, in the present case, it is experimentally difficult to obtain the precise bond lengths among lightweight atoms (C, N) because of the existence of heavy atoms such as Ag and I. Here we employed another method to

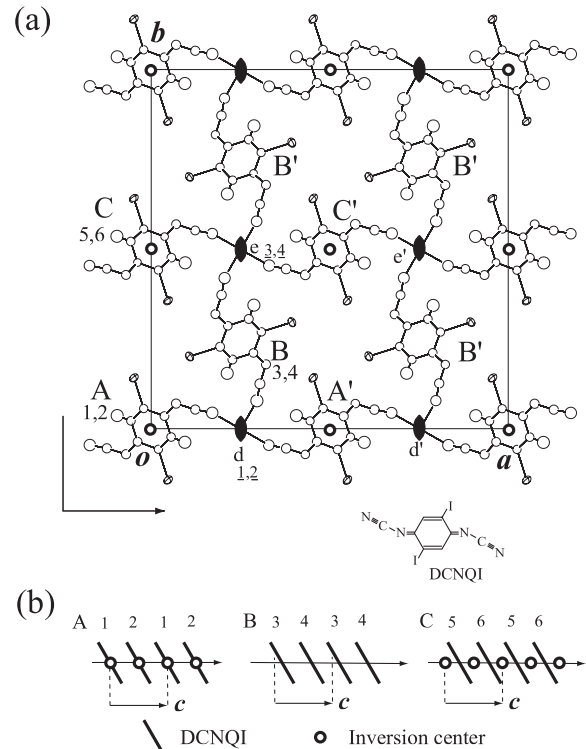


FIG. 1. (a) The structure of  $(\text{DI-DCNQI})_2\text{Ag}$  with space group  $P2/a$  projected to the  $c$  plane. DCNQI molecules labeled 1–6 compose columns A–C, and Ag ions labeled  $\underline{1}$  and  $\underline{2}$  ( $\underline{3}$  and  $\underline{4}$ ) compose column d (e). Inversion centers, twofold rotation axes, and the  $a$ -glide plane are shown by bold open circles, solid symbols, and kinked arrows, respectively. (b) Schematic side view of DCNQI columns A, B, and C. Thick lines depict DCNQI molecules. Relative positions of inversion centers in relation to the molecules on column A are different from that on column C. There is no inversion center on column B.

estimate the valence arrangement based on the displacements of atoms. The displacements of DCNQI molecules and Ag ions along the  $c$  axis are prominent, while those along the  $a$  and the  $b$  axis were negligible. Figure 2(a) shows the displacements of each site from the HT phase structure. The shifts of Ag ions are larger than those of molecules. Figure 2(b) shows schematic figures of local atomic arrangements around the silver ions and their displacement vectors. We determined the spatial charge distribution from the displacement of Ag ions, which is proportional to the electric field modulated by the charge ordering under harmonic approximation. The electron-rich (poor) sites are assigned to molecules 1 and 4 (2 and 3) because Ag cations should shift toward the negative charge area. Therefore, columns A and B are found to be in a CO state. The molecules on column C (DCNQI 5 and 6) must have the same charge because all molecules on this column are equivalent due to the inversion symmetry. The dimerization of the molecules shows that columns B and C are in the bond order wave (BOW) state; column B is in a mixture of CO and BOW states, while column C is in a pure BOW

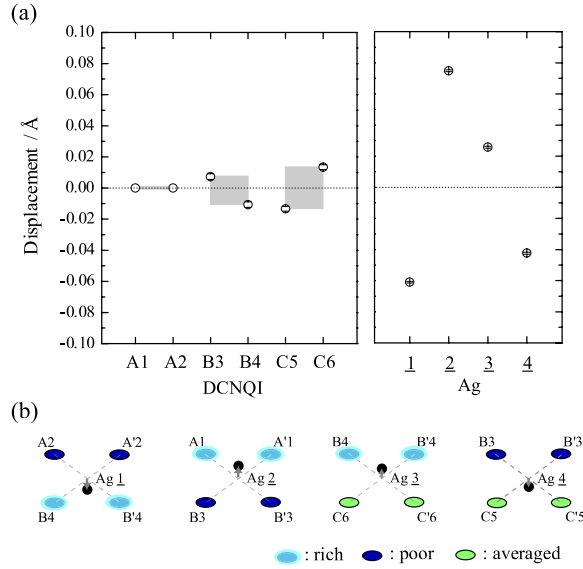


FIG. 2 (color online). (a) Molecular and atomic displacements along the  $c$  axis from the HT phase structure. The numerals in the horizontal axis and A–C labels, respectively, exhibit each site and column defined in Fig. 1. The positions of molecules were defined by the center of gravity of a six-member ring. The rectangular shades are guides to the eye. (b) Schematic figures of the silver ion surrounded by four DCNQI molecules. The gray arrows represent the directions of Ag displacement.

state. This structure, in which three kinds of columns are aligned, is unprecedented for Q1D compounds and differs from any of the previous studies on this compound [8,12].

Based on the molecular displacements, which are proportional to the first derivative of the charge modulation, we derived that the system has CDW columns having different phases in relation to the molecules as shown in Fig. 3(a). This molecular displacement is represented by  $-u \sin(2\pi z - \Phi_i)$ , where  $z$ ,  $u$ , and  $\Phi_i$  are the fractional coordinate in the  $c$  direction, the amplitude of the molecular displacement, and the initial phase of the lattice modulation for column  $i = \{A, B, C\}$ , respectively. The charge modulation of the CDW at position  $z$  is proportional to  $\cos(2\pi z - \Phi_i)$ . For the sake of simplicity, we use a phase parameter  $\phi = (2\pi z - \Phi_i)$ . In column A, a CO without lattice displacement is established. Using the valence arrangement shown in Fig. 2(b), the  $\Phi_A$  is found to be zero. A BOW with dimerization is established in column C', meaning that all molecules are on the node of the CDW. The  $\Phi_C$  is zero so that the directions of the molecular displacements shown in Fig. 2(a) are reproduced. In column B, which has two molecules at  $z = 1/8$  and  $5/8$ , mixed states of CO and BOW are established. The phase of the CDW at the molecule is intermediate. The magnitude of the molecular displacement on column B is 67% of that on column C. The phase  $\phi = \sin^{-1}(\pm 0.67) \approx \pi(1/4 + n)$ ; therefore,  $\Phi_B = \pi$ . Here, we used both the direction of the molecular displacement and valence arrangement for

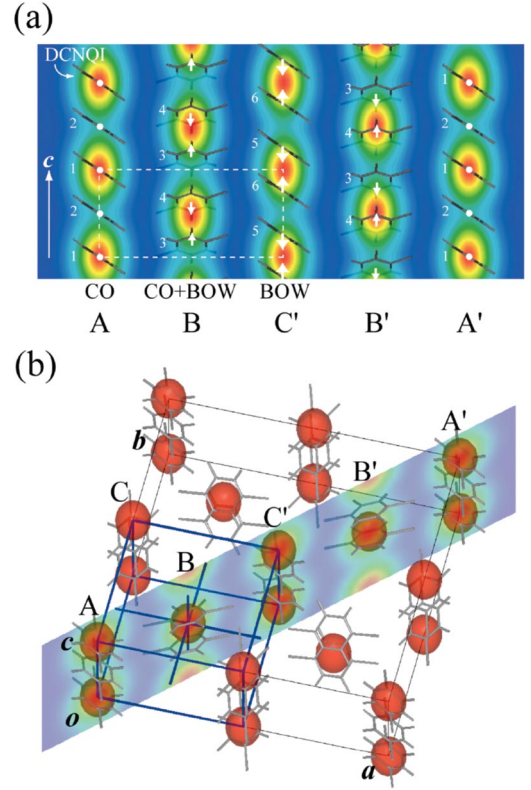


FIG. 3 (color). Schematic view of the molecules and charge density waves. (a) Relationship between molecules and charge density waves on each column. Red areas depict electron-rich areas. The arrows show the directions of molecular displacements. (b) Three-dimensional view of the Wigner crystal-type charge arrangement and the molecules. Charge-rich areas are shown by red ellipses, forming a body-centered tetragonal lattice drawn by the blue lines.

choosing the sign of the phase. Figure 3(b) shows the schematic CDW arrangement in the unit cell of the LT phase of  $(DI\text{-}DCNQI)_2\text{Ag}$ , in which the charge-rich areas are depicted by spheres. The charge-rich area forms a body-centered tetragonal lattice with a unit cell of  $a_p/2 \times b_p/2 \times 2c_p$ . This charge structure reminds us the Wigner crystal in which the electrons repel each other. In this system, the origin of this structure is electron-electron interaction and the electron-lattice interaction is negligible, because the CDW phase is not locked to the lattice. Therefore, we conclude that this electronic structure is caused by the Wigner crystallization.

In general, for Wigner crystallization to occur it is necessary that electron density is sufficiently low to allow the Coulomb interaction to be dominant compared with the kinetic energy [17], and it is considered that the electrons of common materials are too dense to form the Wigner crystal. The Wigner crystallization in this material is likely due to the suppression of kinematic energy in the narrow band. Recent theoretical work on the jellium model [18] has shown that Wigner crystallization is enhanced in low-

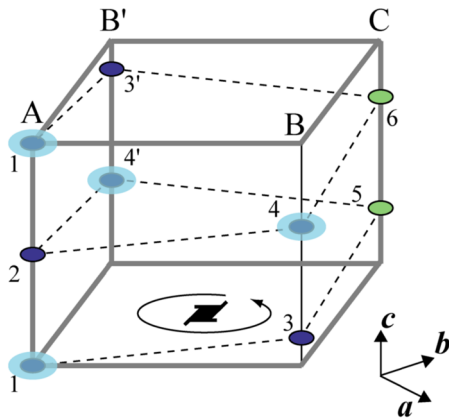


FIG. 4 (color online). Schematic figure of helical structure along with the A, B, C, B', and A columns of Fig. 1. Molecular indices are the same as that in Fig. 1. First neighbor site is on the same chain, and the dashed lines connect second nearest neighbor molecules.

dimensional solids because the kinetic energy is suppressed by this dimensionality, and consequently the relative Coulomb effect is emphasized. According to this theory,  $(\text{DI-DCNQI})_2\text{Ag}$  could be a Wigner crystal.

Finally, we discuss the origin of the columns having different electronic structure. Most Q1D systems have only one kind of chains, and the 3D ordering binds such chains so that the sum of  $E_V$  reaches a minimum, where  $E_V$  is the interchain Coulomb energy summed over one chain. By contrast, this system has three kinds of columns. This unconventional state of chains may be caused by the geometrical frustration of the  $(\text{DCNQI})_2\text{Ag}$  structure: If all chains have the same CO arrangement, the 3D order having the same  $E_V$  for all chains cannot be achieved. The key structure is not a triangle lattice but the fourfold screw symmetry. According to several studies [2,19], the interchain Coulomb interaction  $V$  is not significantly weak, and a positive  $V$  favors the alternating charge arrangement between the columns. Let us arrange the charge ordered columns to minimize the Coulomb energy. Figure 4 shows a schematic view of columns A, B, C, and B'; the interchain interaction  $V$  works between two molecules connected by the dashed lines. The valence arrangement in column A is {1:rich, 2:poor}, and it determines the valences in B and B' to be {3:poor, 4:rich} and {3':poor, 4':rich}. This condition is summarized in Fig. 4. So far, the arrangement is unique. However, the valence of column C cannot be determined in this manner. Molecule 5 has molecules 3 and 4' as its relevant neighbors, whose valence is poor and rich, respectively. Molecule 6 has the same condition. The charge arrangement is frustrated, and the observed BOW chain relaxes this frustration by allowing fractional valences on each molecule.

In summary, we have conducted a low-temperature structure analysis of  $(\text{DI-DCNQI})_2\text{Ag}$  and clarified its un-

conventional valence arrangement, which could be related to geometrical frustration. This charge arrangement is interpreted as the Wigner crystal.

The authors are grateful to Professor K. Yakushi and Dr. H. Seo for their fruitful discussions. This work was supported by a Grant-in-Aid for Creative Scientific Research and Scientific Research from the Ministry of Education, Culture, Sports, Science, and Technology of Japan.

\*Corresponding author.

†Present address: Graduate School of Human and Environmental Studies, Kyoto University, Kyoto 606-8501, Japan.

- [1] R. E. Peierls, *Quantum Theory of Solids* (Clarendon, Oxford, 1955).
- [2] H. Seo, C. Hotta, and H. Fukuyama, *Chem. Rev.* **104**, 5005 (2004), and references therein.
- [3] T. Miyazaki, K. Terakura, Y. Morikawa, and T. Yamasaki, *Phys. Rev. Lett.* **74**, 5104 (1995).
- [4] H.-P. Werner, J. U. von Schütz, H. C. Wolf, R. Kremer, M. Gehrke, A. Aumüller, P. Erk, and S. Hünig, *Solid State Commun.* **65**, 809 (1988).
- [5] K. Hiraki and K. Kanoda, *Phys. Rev. B* **54**, R17276 (1996).
- [6] R. Moret, P. Erk, S. Hünig, and J. U. Von Schütz, *J. Phys. (France)* **49**, 1925 (1988).
- [7] Y. Nogami, K. Oshima, K. Hiraki, and K. Kanoda, *J. Phys. IV* **9**, 357 (1999).
- [8] K. Hiraki and K. Kanoda, *Phys. Rev. Lett.* **80**, 4737 (1998).
- [9] T. Sakurai, N. Nakagawa, S. Okubo, H. Ohta, K. Kanoda, and K. Hiraki, *J. Phys. Soc. Jpn.* **70**, 1794 (2001).
- [10] H. Seo and H. Fukuyama, *J. Phys. Soc. Jpn.* **66**, 1249 (1997).
- [11] R. Kato, H. Kobayashi, and A. Kobayashi, *J. Am. Chem. Soc.* **111**, 5224 (1989).
- [12] K. Yamamoto, T. Yamamoto, K. Yakushi, C. Pecile, and M. Meneghetti, *Phys. Rev. B* **71**, 045118 (2005).
- [13] The intensity distribution of superlattice reflections also indicated the possibility of inversion symmetry, where we used Wilson's statistical method: A. J. C. Wilson, *Acta Crystallogr.* **2**, 318 (1949).
- [14] The intensity of the Bragg reflections was measured in a half-sphere of reciprocal space in the range  $2\theta < 100^\circ$ . The number of unique reflections was 28 177. SHELX97 software was used for refinements. Silver and iodine atoms were anisotropically refined.
- [15] *International Tables for Crystallography*, edited by U. Shmueli (Kluwer, Dordrecht, 2001), Vol. B
- [16] P. Guionneau, C. J. Kepert, G. Bravic, D. Chasseau, M. R. Truter, M. Kurmoo, and P. Day, *Synth. Met.* **86**, 1973 (1997).
- [17] E. Wigner, *Phys. Rev.* **46**, 1002 (1934).
- [18] G. Rastelli, P. Quémerais, and S. Fratini, *Phys. Rev. B* **73**, 155103 (2006).
- [19] H. Seo, J. Merino, H. Yoshioka, and M. Ogata, *J. Phys. Soc. Jpn.* **75**, 051009 (2006).